An Active-Passive Microwave Land Surface Database from GPM

S. Joseph Munchak[1]*, Sarah Ringerud[1,2], Yalei You[2], and Ludovic Brucker[1,3]

1: NASA Goddard Space Flight Center; 2:ESSIC, 3:USRA *s.j.munchak@nasa.gov

1DVAR Atmosphere/Surface Retrieval

GMI observations contain information about the atmospheric temperature and water vapor profile and surface emissivity, in addition to clouds and precipitation. In clear-sky conditions, the information content pertaining to the surface and atmospheric profile is high. To develop databases of surface characteristics for use in all-sky retrievals, we have developed a 1DVAR clear-sky retrieval for use with GPM data. One unique aspect of our approach is the use of error covariance (and corresponding error EOFs; shown on the right) derived from comparisons of MERRA2 reanalyses and radiosonde observations. With these error structures, we begin with the MERRA2 data as the first guess and allow the retrieval to adjust the temperature and water vapor profiles within the bounds implied by these error covariances using an optimal estimation technique. This is superior to using climatological variability or a climatological first guess, as shown below. For computational efficiency, only the first 5 EOFs are retrieved. This is where the residual error in brightness temperature becomes similar to the channel noise.

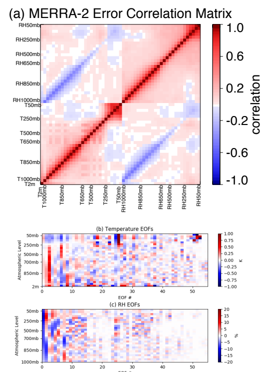

An example retrieval is shown below, comparing three different representations of the a priori atmospheric state and its error covariance. This case contained both synoptic-scale precipitation associated with a cold front and lake-effect snowbands over the northeast United State on 9 January 2015. The first row shows the retrieval using climatological first guess and covariance (CLIM/CLIM). The retrieval correctly reduces the column water vapor to reduce the brightness temperature error, but incorrectly attributes the cold Tbs in the snow bands to a combination of very low water vapor and low surface emissivity. The second row uses the MERRA2 atmospheric state as the first guess, with the climatological error covariance (MERRA2/CLIM). The posterior brightness temperature error is reduced and the retrieved column water vapor more closely resembles the MERRA2 field, but regions of precipitation are still incorrectly attributed to low TPW and low emissivity. In the third row, the retrieval using MERRA2 for both the first guess and error covariance is shown, and this retrieval does the best job of correctly filtering out the precipitation-affected observations while still modifying the clear-sky profiles to be consistent with the information contained in the GMI observations.

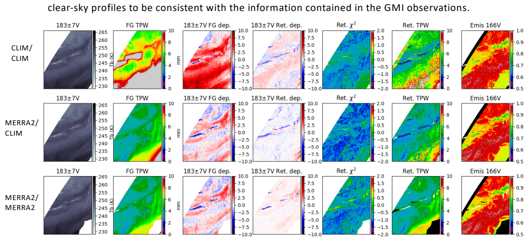

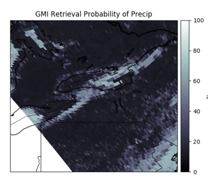

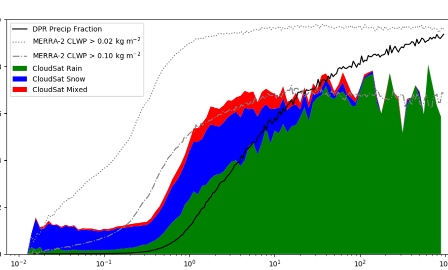

The retrieval normalized cost (Φ_N), which represents the departure of the retrieved state from the first guess and the simulated from actual observations, can be used to assess the probability of precipitation. On the left, the DPR precipitation probability (black solid line) is shown as a function of Φ_N, generally increasing once Φ_N exceeds 1. The GPM-CloudSat matched observations are also uses to assess the ability of GMI to detect precipitation that is lighter than the DPR detectability threshold. We note that the probability of CloudSat-detected precipitation begins to increase at lower Φ_N values than DPR-detected precipitation, affirming that GMI can indeed detect precipitation that DPR cannot, and these values are used to convert the Φ_N from the lake effect snow case to precipitation probability above. We also note that some light precipitation, predominantly snow, cannot be detected by GMI using any Φ_N threshold. The impact of liquid clouds (which are not accounted for in this retrieval over land surfaces) is also examined using MERRA2. The occurrence of 0.02 and 0.1 kg/m^2 liquid water path clouds also increases as a function of Φ_N, indicating some potential for this method to detect liquid clouds over land as well.

Reference: Munchak, S. J., S. Ringerud, L. Brucker, Y. You, I. de Gelis, and C. Prigent (2019). An Active-Passive Microwave Land Surface Database from GPM. *In revision, IEEE Transactions on Geoscience and Remote Sensing*

Surface Emissivity/Backscatter Classification

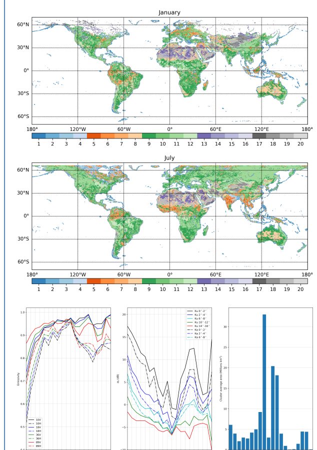

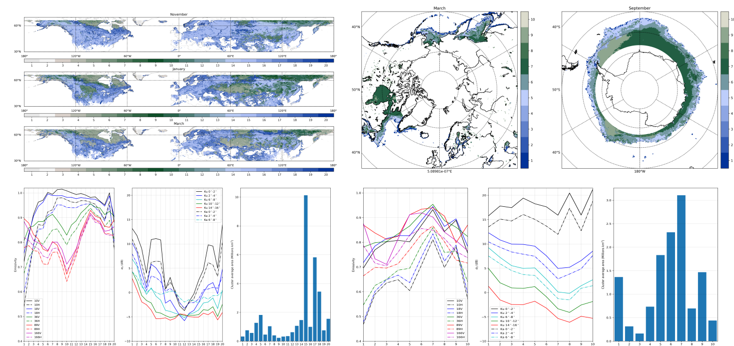

A Kohonen Self-Organizing Map clustering technique is used to classify surfaces based on their emissivity and backscatter properties. Separate classifications were performed for non-snow-covered land (left), snow-covered land (middle), and sea ice (right). These classes reveal the gradation of surface properties as vegetation, inundated area, surface roughness, and surface composition changes. The snow classes have a strong seasonal dependence, as as snowpack water equivalent and grain size evolve throughout the season, eventually melting. Likewise, sea ice expands in concentration and accumulates snow throughout the winter before melt ponds eventually form. These surface classifications will be used in an upcoming version of the GPM Combined Algorithm.

Applications: Sensitivity to Accumulated Rain & Snow

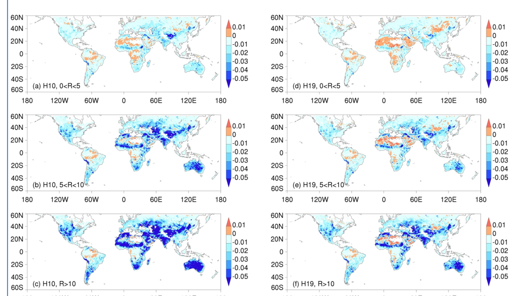

The GMI surface emissivity database is used to examine the sensitivity of emissivity to rainfall by comparing observations after dry periods with those after various amounts of rain have fallen. The 10 and 19 GHz horizontally-polarized emissivities are most sensitive to rainfall over surfaces with low to moderate amounts of vegetation, with strong decreases in emissivity in proportion to the amount of rainfall. Curiously, some desert surfaces appear to increase in emissivity after rain events, a phenomenon which is currently being explored. For more information, see poster 241 by Yalei You, “Daily Rainfall Estimate by Emissivity Temporal Variation from 10 Satellites”

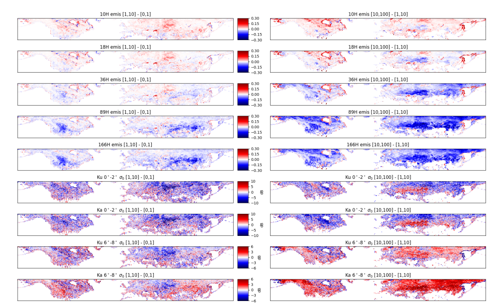

The response of surface emissivity and backscatter to snowfall is examined above. We compared the emissivity and backscatter when minimal (0-1 mm), moderate (1-10 mm), and large (10-100mm) amounts of snow water equivalent (SWE) were present, using MERRA2 reanalysis. The 89 and 166 GHz channels are most sensitive to increases from minimal to moderate SWE, whereas the 36 GHz channel is sensitive to larger amounts. The backscatter response depends on incidence angle and frequency – near-nadir backscatter decreases with SWE over most surfaces, but off-nadir backscatter increases, with effects more pronounced at Ka band than Ku band. Both emissivity and backscatter responses to snowfall also show a strong dependence on the underlying surface type after controlling for SWE amount.